Self-Sustained Motion of a Train of Haptotactic Microcapsules

ARTICLE *in* LANGMUIR · OCTOBER 2009

Impact Factor: 4.46 · DOI: 10.1021/la9017823 · Source: PubMed

4 AUTHORS, INCLUDING:

Amitabh Bhattacharya
University of Pittsburgh
41 PUBLICATIONS **147** CITATIONS
SEE PROFILE

Berk Usta
Massachusetts General Hospital
48 PUBLICATIONS **434** CITATIONS
SEE PROFILE

Victor V. Yashin
University of Pittsburgh
83 PUBLICATIONS **825** CITATIONS
SEE PROFILE

Langmuir Letter

pubs.acs.org/Langmuir

Self-Sustained Motion of a Train of Haptotactic Microcapsules

Amitabh Bhattacharya, O. Berk Usta, Victor V. Yashin, and Anna C. Balazs*

Chemical Engineering Department, University of Pittsburgh, Pittsburgh, Pennsylvania 15261

Received May 19, 2009. Revised Manuscript Received July 16, 2009

Using theory and simulation, we design a "train" of N microcapsules that undergoes self-sustained, directed motion along an adhesive surface in solution. The motion is initiated by the release of nanoparticles from a single "signaling" capsule at one end of the train. The released nanoparticles can bind to the underlying surface and thereby induce an adhesion gradient on the substrate. Through the combined effects of the self-imposed adhesion gradient and hydrodynamic interactions, the N microcapsules autonomously move in single file toward the region of greatest adhesion. At late times, this train reaches a steady-state velocity U, which decreases with train length as $N^{-1/2}$. We calculate the maximum length for which the train maintains this cooperative, autonomous motion.

Biological cells are commonly recruited to specific locations through an adhesion gradient on an underlying surface. In this process, referred to as haptotaxis, enthalpic interactions drive the cells to move toward the more attractive or adhesive regions of the substrate. In the latter scenario, the adhesion gradient is already in place as the cell begins its migration. In systems involving synthetic vesicles or microcapsules, however, the adhesion gradient can be created dynamically as, for example, these carriers release reagents, which modify the wetting properties of the substrate.[1,2] Because the capsules introduce their own evolving adhesion gradient, they can undergo a self-induced haptotactic motion.[3]

Moving in a fluid, such self-propelled capsules generate hydrodynamic flows, which can affect the motion of nearby species.[2] Herein, we use theory and simulation to design a system of motile microcapsules where the combination of a self-imposed adhesion gradient and hydrodynamic interactions causes an entire train of N capsules to undergo self-directed movement. The "signaling" capsule (on the left in Figure 1a), which is localized on a surface, emits nanoparticles that bind to the surface and thereby create the adhesion gradient. The "target" capsules to the right of this carrier start moving because of the gradient. Their movement, however, generates a flow that pulls the signaling capsule onto the adhesion gradient so that the whole row of capsules undergoes spontaneous motion. Surprisingly, as we show below, a single signaling microcarrier is sufficiently powerful that it can effectively propel a relatively long train. Furthermore, the speed of this train, U, decreases relatively slowly with the number of capsules. These findings reveal that the introduction of a single "organizing center" (i.e., the signaling capsule) into an ensemble of otherwise identical colloids can give rise to distinctive forms of collective behavior.

In our system, a line of N initially stationary capsules is localized on an adhesive surface in a fluid-filled channel, which has a height H (Figure 1a). Each capsule has an outer radius R, and the initial, uniform separation between the centers of these capsules is $2.3R$. The signaling capsule at the left end of this train contains a dispersion of nanoparticles in its fluid-filled core, whereas the target capsules contain only fluid. To probe the behavior of this 2D system, we first use a numerical simulation that integrates the coupled motion of the fluids, capsules, and nanoparticles. The dynamics of the host and encapsulated fluids are captured through the lattice Boltzmann model (LBM),[4] which is an efficient solver for the Navier−Stokes equation. The velocity field of the fluid is periodic in x and satisfies the no-slip boundary conditions at the walls and surface of the capsules. The motion of each capsule is simulated using rigid body dynamics. The host and internal fluids interact with the capsules' rigid shells through appropriate boundary conditions.[5,6] In particular, the shell imposes its momentum on the surrounding fluids through the corresponding velocity distributions in the LBM. In turn, the capsules experience forces due to the fluid pressure and viscous stresses at the interfaces. To prevent overlap between neighboring capsules, a repulsive, short-range, pairwise potential interaction is introduced between the nodes of these capsules.

We integrate the above approach with a continuum model for the diffusion of nanoparticles, which emanate from a point source at the center of the signaling capsule (i.e., at $(x_{sig}(t), y_{sig}(t))$. These particles are released at a constant rate specified by S (particles/time) and are assumed to undergo Brownian motion in the solid and fluid phases without imparting any momentum to the fluid or solid. This is a reasonable assumption, provided the solid capsule shells are porous and the volume fraction of nanoparticles is small. The concentration field of nanoparticles, $c(x, y, t)$ particles/area, satisfies the advection−diffusion equation. Here, we assume that the diffusivity of nanoparticles in the solid and fluid phase is characterized by the same value D. The simulations were performed at low Peclet number, $\mathrm{Pe} = UR/D \ll 1$, and low Reynolds number, $\mathrm{Re} = \rho UR/\mu \ll 1$, where ρ and μ are the respective fluid density and viscosity.

The released nanoparticles bind to the top and bottom walls of the channel. We further specify that the surface coverage of nanoparticles at a point x on the bottom wall is $c_s(x, t)$

*Corresponding author. E-mail: balazs@pitt.edu.

(1) (a) Dos Santos, F. D.; Ondarçuhu, T. *Phys. Rev. Lett.* **1995**, *75*, 2972–2975. (b) Durand, I.; Jonson, P.; Misbah, C; Valance, A.; Kassner, K. *Phys. Rev. E* **1997**, *56*, R3776–R3779. (c) Lee, S. W.; Kwok, D. Y.; Laibinis, P. E. *Phys. Rev. E* **2002**, *65*, 051602. (d) Sumino, Y.; Magome, N.; Hamada, T; Yoshikawa, K. *Phys. Rev. Lett.* **2005**, *94*, 068301.

(2) Usta, O. B.; Alexeev, A.; Zhu, G.; Balazs, A. C. *ACS Nano* **2008**, *2*, 471–476.

(3) Solon, J.; Streicher, P.; Richter, R.; Brochard-Wyart, F.; Bassereau, P. *Proc. Nat. Acad. Sci. U.S.A.* **2006**, *103*, 12382–12387.

(4) Succi, S. *The Lattice Boltzmann Equation for Fluid Dynamics and Beyond*; Oxford University Press: Oxford, U.K., 2001.

(5) Alexeev, A.; Verberg, R.; Balazs, A. C. *Macromolecules* **2005**, *38*, 10244–10260.

(6) Bouzidi, M.; Firdaouss, M.; Lallemand, P. *Phys. Fluids* **2001**, *13*, 3452–3459.

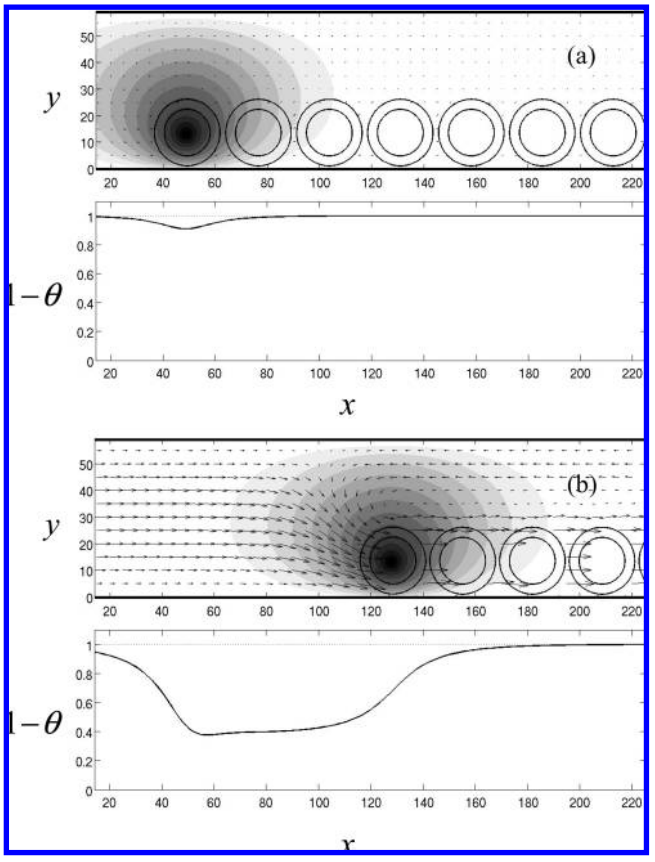

Figure 1. Snapshots of the 2D capsule train with $N = 8$ at time (a) $t = 1 \times 10^4$ LBM time steps (early time) and (b) $t = 2 \times 10^5$ LBM time steps (at steady state). The snapshots are truncated on the left and right. (Top panels) Capsules are shown as annular disks. The first capsule from the left, with a point source of nanoparticles (S) at its center, is the signaling capsule, followed by empty target capsules to its right. Shaded isocontours show the concentration field of nanoparticles, $c(x, y, t)$. The vector plot represents the velocity field induced in the fluid by the moving train. (Bottom panels) Fraction of unoccupied sites on the substrate $1 - \theta$ (bold line) and reference (dotted line) line denoting zero coverage fraction $\theta = 0$.

particles/length, and the maximum possible coverage (or saturation coverage) of nanoparticles at each site is c_s^{max}. Thus, $\theta(x, t) = c_s(x, t)/c_s^{max}$ is the fractional coverage of nanoparticles on the bottom wall. The top wall is a perfectly adsorbing surface, implying the boundary condition $c(x, H, t) = 0$. However, the bottom wall is a chemisorbing substrate, so the rate of adsorption of nanoparticles at x is proportional to both $c(x, 0, t)$ and the fraction of unoccupied reactive sites $[1 - \theta(x, t)]$. This implies a boundary condition $D\partial_y c|_{y=0} = k_r c(x, 0, t)[1 - \theta(x, t)]$, where k_r is the reaction rate constant (having the physical dimensions of length/time). To compute θ, we observe that the rate of change in coverage at the lower wall is equal to the flux of adsorbed nanoparticles:

$$\frac{\partial c_s(x,t)}{\partial t} = D\frac{\partial c}{\partial y}\Big|_{y=0} \qquad (1)$$

The solution of eq 1, along with the chemisorption boundary condition for c, ensures that the nanoparticles do not adsorb at the saturated parts of the substrate. The equations for $c(x, y, t)$ and $c_s(x, t)$ are simulated using standard finite-difference methods,[7] with initial condition $c(x, y, 0) = c_s(x, 0) = 0$.

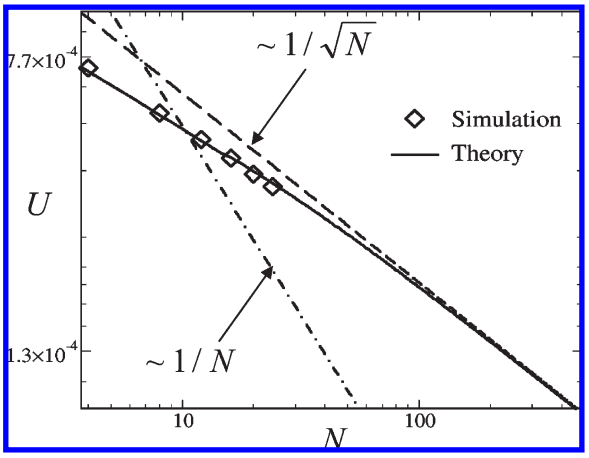

Figure 2. Comparison of U vs N behavior predicted by simulation and analytical solution (eq 6) at $c_s^{max} = 8000$, along with reference lines for $1/N$ and $1/\sqrt{N}$ behavior. The other parameters are $S = 3$, $\mu = 1/6$, $R = 12.5$, $H = 60$, $D = 0.1$, and $k_r = 1$. The analytical solution uses $\eta = 1.03$, which was measured from simulations. The LBM time step and LBM grid size are used as units for time and length, respectively.

The chemisorbed nanoparticles are assumed to modify the adhesive properties of the surface, decreasing the attraction between the capsule and substrate. Specifically, the adhesive force between the capsules and the substrate is characterized by the following Morse potential: $\varphi(x, r, t) = \varepsilon(x, t)\{1 - \exp[-(r - r_0)/\kappa]\}^2$. Here, φ is the energy of interaction between a capsule surface node at $(x + r_x, r_y)$ and a wall node at $(x, 0)$. The adhesion strength, ε, is a linearly decreasing function of $\theta(x, t)$ so that $\varepsilon(x, t) = \varepsilon_{sat} + \varepsilon_0[1 - \theta(x, t)]$ with ε_{sat}, $\varepsilon_0 > 0$. Thus, a nonuniform fractional coverage induces a corresponding variation in adhesion strength.

Our simulations reveal that, for a range of N, the train starts moving if the value of c_s^{max} is sufficiently large (~3000−8000 particles/length) and the signaling capsule is sufficiently close to the first target capsule. Given a steady nanoparticle release rate S, the system eventually reaches a state where both the adhesion gradient and the train move with a steady velocity U along the substrate (Figure 1b). At this velocity, the net propulsive force acting on the train due to the adhesion gradient balances the net drag force due to the surrounding fluid.

From Figure 2, we see that the velocity U decreases monotonically with increasing N. Above a certain value of N, the motion can no longer be sustained, and the train comes to a halt. Figure 1b shows that the adhesion gradient underneath each capsule decreases rapidly from the signaling end; consequently, essentially all of the propulsive force acts on the first few capsules. Hence, for long trains, the net propulsive force is independent of N. If we also assume the propulsive force to be independent of U and the drag force on a long train to be approximately proportional to NU, then by balancing the forces on the train we would obtain $U \propto N^{-1}$. Our simulations, however, show that U decreases much more slowly than $1/N$ (Figure 2). Below, we derive an analytical model to demonstrate that the correct asymptotic behavior is $U \propto N^{-1/2}$ and subsequently determine the maximum length of a self-propelled train.

To calculate steady-state velocity U, we must establish the net drag force on the train due to fluid flow, F_D, and the net propulsion force on the train due to adhesion, F_A. In the Stokes flow regime, for a fixed value of R/H, the drag force is $F_D = \mu U R f(N)$.[8]

(7) Moin, P. *Engineering Numerical Analysis*; Cambridge University Press: Cambridge, U.K., 2001; p 93.

(8) Happel, J; Brenner, H. *Low Reynolds Number Hydrodynamics*; Prentice-Hall: Englewood Cliffs, NJ, 1965; p 115.

We also observe that for $N \gg H/2R$ the local flow fields centered around any two capsules situated away from the ends of the train are identical (Figure 1b). The structure of this local flow field is independent of the length of the train. As a result, the drag per capsule, F_D/N, is constant for long trains, leading to the conclusion that $f \propto N$ for large N. We calibrate $f(N)$ using a separate set of simulations, where we set $S = 0$, vary N from 2 to 24, and push the train by applying a constant external force on the signaling capsule. The following composite best fit for f, obtained at $R/H = 0.21$, completes the semiempirical model for F_D:

$$f = \begin{cases} d_0 + d_1 N, N \geq N^* \\ d_2 N^{\gamma}, N < N^* \end{cases} \quad (2)$$

Here, $\gamma = 0.78$, $N^* = 16$, $d_0 = 9.3$, $d_1 = 1.2$, and $d_2 = 3.3$.

The force due to the adhesion gradient, $A_i(t)$, acting on the ith capsule in the train (counting from the signaling end) located at x_i is linearly proportional to $\partial_x \varepsilon|_{x=x_i}$.[9] It follows that $A_i(t) = -[\eta/c_s^{max}]\partial_x c_s|_{x=x_i}$, where η is a constant that depends on R, ε_0, κ, and r_0. Coverage profile $c_s(x, t)$ is solved in tandem with the nanoparticle concentration field $c(x, y, t)$ using eq 1. At steady velocity, both $c(x, y, t)$ and $c_s(x, t)$ are stationary in the coordinate frame $(X, Y) = (x - Ut, y)$, which moves with the train. We use the notation $c(x, y, t) = C(X, Y)$ and $c(x, t) = C_s(X)$ and fix the signaling capsule at $X = 0$. At low Peclet number, the advection terms in the advection-diffusion equation satisfied by $C(X, Y)$ can be omitted, and we need to solve only the Poisson equation $D[\partial_X^2 + \partial_Y^2]C = -S\delta(X)\,\delta(Y - R)$. In the latter equation, we fixed $y_{sig} = R$, neglecting capsule-wall separation (~1 LBM unit in simulations). The perfect adsorption of nanoparticles at the top wall implies the boundary condition $C(X, H) = 0$. The chemisorption boundary condition at the lower wall is simplified by noting that in our simulations $k_r R \gg D$, implying that the chemisorption is limited by the diffusion of nanoparticles to the surface. Thus, $C(X, 0) \approx 0$ if the substrate is not saturated at X. Furthermore, the substrate underneath a moving train (i.e., for all $X \geq 0$ if U is positive) must be unsaturated for an adhesion gradient to exist under all the capsules. A saturated patch on the substrate, located behind the train, will have little effect on $C(X, Y)$ at any $X \geq 0$. Thus, $C(X, 0) = 0$ is used, for all X, to approximate the chemisorption boundary condition. We solve the Poisson equation for $C(X, Y)$, satisfying the zero Dirichlet boundary conditions at both surfaces in terms of appropriate eigenfunctions.[10] Equation 1 is then utilized to obtain $C_s(X)$ as

$$C_s(X) = -\frac{1}{U}\int_X^{\infty} J(X')\,dX' \quad (3)$$

where $J(X) = -D\partial_Y C|_{Y=0}$. The limit $C_s(\infty) = 0$ has been taken into account in eq 3.

Because of the low Peclet number, $C(X, Y)$ does not depend on U. As a result, the flux J is also independent of U. This leads, via eq 3, to the scaling $C_s(X) \propto U^{-1}$. This scaling arises because a faster train causes proportionally fewer nanoparticles per unit length to adsorb onto the substrate. Equation 3, however, does not constrain C_s to be less than c_s^{max} because we approximated the chemisorption at the lower wall with a zero Dirichlet boundary condition. We impose the constraint by truncating the solution of eq 3

$$C_s(X) = \min\left[S(\pi U)^{-1}(g(\infty) - g(X)), c_s^{max}\right] \quad (4)$$

(9) Alexeev, A.; Balazs, A. C. *Soft Matter* **2007**, *3*, 1500–1505.
(10) Butkov, E. *Mathematical Physics*; Addison-Wesley: Reading, MA, 1968; p 552.

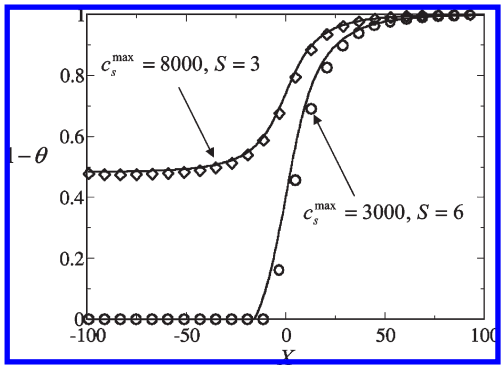

Figure 3. Comparison of profiles for fraction of unoccupied sites on the lower substrate predicted by theory (lines) and simulation (symbols) for $N = 8$ at steady state. The substrate can be partially saturated ($c_s^{max} = 3000$, $S = 6$) or completely unsaturated ($c_s^{max} = 8000$, $S = 3$). The other parameters are as listed in Figure 2.

where $g(X) = \tan^{-1}[\cot(\pi R/2H)\tanh(\pi X/2H)]$.

We can now obtain the total adhesive force acting on a moving train, F_A, through the summation $F_A = \Sigma^N{}_{i=1} A_i(t)$. Neglecting the space between capsules, we can write $X_i = x_i - Ut = 2R(i - 1)$, yielding

$$F_A = \frac{\eta S}{2UHc_s{}^{max}}\Gamma\left(N, \frac{R}{H}\right) \quad (5)$$

where $\Gamma = \sin(R\pi/H)\Sigma^N{}_{i=1}[\cosh(2(i-1)R\pi/H) - \cos(R\pi/H)]^{-1}$ converges rapidly with N. Equation 5 indicates that the propulsion force, F_A, is independent of N for $N \gg 1$ while being proportional to U^{-1}.

This brings us to the central result of the paper. Because $F_D \propto NU$ and also $F_A \propto U^{-1}$ at large N, equating F_D to F_A implies that $U \propto N^{-1/2}$. Using eqs 2 and 5, we can also solve for U at all N to obtain

$$U = \left[\frac{\eta S}{2\mu Hc_s{}^{max} f(N)}\Gamma\left(N, \frac{R}{H}\right)\right]^{1/2} \quad (6)$$

Figure 2 reveals that the values of U calculated from eq 6 are in excellent agreement with simulations. Figure 3 shows that the coverage profile, $C_s(X)$, calculated using eqs 4 and 6 also agrees well with simulations, even when the substrate is partially saturated.

We can now estimate the maximum number of capsules that can be self-propelled. We first note that increasing the length of the train decreases U (eq 6) and therefore brings $C_s(0)$ closer to saturation (eq 4). Also, the train cannot maintain a sustained velocity if the adhesion gradient underneath the signaling capsule vanishes; it stays self-propelled as long as $C_s(0) < c_s^{max}$. For cases where $C_s(0) < c_s^{max}$ occurs at a large N, eqs 4 and 6 yield the following upper limit for N: $N < \pi^2\eta c_s^{max}\,\Gamma(\infty, R/H)\,[2\mu SHd_1 g(\infty)^2]^{-1}$. For wide channels, with $R/H \ll 1$, this limit is simplified to $N < [1.73\eta c_s^{max}(\mu RSd_1)^2]^{-1}$. Thus, various parameters can be altered in order to ensure the self-propulsion of a long train of capsules.

In conclusion, we showed that a train of microcapsules localized on an adhesive surface in solution could be driven to undergo self-propelled motion by a single "signaling" capsule. A crucial step in our analysis was deriving the relationships $F_D \propto NU$ and $F_A \propto U^{-1}$. The latter scaling follows from the fact that a slower train provides a higher surface coverage of nanoparticles.

Consequently, we found that the velocity of the train decreases as $N^{-1/2}$, which is borne out by the simulations. This scenario could potentially be useful for microfluidic applications, where a particle-filled microcapsule could be harnessed to push a "cargo" (i.e., other capsules or cells) through the device. Remarkably, increasing the length of this cargo would not entail dramatic decreases in speed. To realize this system, we note that that the microcapsules could be confined to a narrow groove or adhesive strip. In future work, we will examine a comparable system in 3D, where we expect to uncover a rich set of collective phenomenon[11] as the signaling and target microcapsules move on a plane.

Acknowledgment. We gratefully acknowledge financial support from the DOE (for partial support of A.B. and O.B.U) and ONR (for partial support of V.V.Y.).

(11) Baron, M.; Blawzdziewicz, J.; Wajnryb, E. *Phys. Rev. Lett.* **2008**, *100*, 174502.